Acute loss of Cell–Cell Communication Caused by G Protein–coupled Receptors: A Critical Role for c-Src

Friso R. Postma, Trudi Hengeveld, Jacqueline Alblas, Ben N.G. Giepmans, Gerben C.M. Zondag, Kees Jalink, and Wouter H. Moolenaar

The Netherlands Cancer Institute, Division of Cellular Biochemistry, 1066 CX Amsterdam, The Netherlands

Abstract. Gap junctions mediate cell–cell communication in almost all tissues, but little is known about their regulation by physiological stimuli. Using a novel single-electrode technique, together with dye coupling studies, we show that in cells expressing gap junction protein connexin43, cell–cell communication is rapidly disrupted by G protein–coupled receptor agonists, notably lysophosphatidic acid, thrombin, and neuropeptides. In the continuous presence of agonist, junctional communication fully recovers within 1–2 h of receptor stimulation. In contrast, a desensitization-defective G protein–coupled receptor mediates prolonged uncoupling, indicating that recovery of communication is controlled, at least in part, by receptor desensitization. Agonist-induced gap junction closure consistently follows inositol lipid breakdown and membrane depolarization and coincides with Rho-mediated cytoskeletal remodeling. However, we find that gap junction closure is independent of Ca^{2+}, protein kinase C, mitogen-activated protein kinase, or membrane potential, and requires neither Rho nor Ras activation. Gap junction closure is prevented by tyrphostins, by dominant-negative c-Src, and in Src-deficient cells. Thus, G protein–coupled receptors use a Src tyrosine kinase pathway to transiently inhibit connexin43-based cell–cell communication.

COMMUNICATION between adjacent cells through gap junction channels occurs in almost all tissues and is fundamental to coordinated cell behavior. In excitable tissues, such as cardiac muscle and neurons, gap junctions allow rapid and synchronous propagation of action potentials. More in general, junctional communication has been implicated in the control of cell proliferation, embryonic development, and tumor suppression (for reviews see Bennett et al., 1991; Beyer, 1993; Hotz-Wagenblatt and Shalloway, 1993; Paul, 1995; Mesnil et al., 1995; Goodenough et al., 1996). Gap junction channels are permeable to small (<1 kD) molecules, including second messengers such as Ca^{2+}, inositol phosphates, and cyclic nucleotides. The integral membrane proteins forming these channels are termed connexins, which are encoded by a multigene family (Bennett et al., 1991; Goodenough et al., 1996; Kumar and Gilula, 1996). Connexin43 (Cx43)[1] is the most widespread and abundant member of this family.

While much has been learned in recent years about the cellular and molecular biology of gap junction channels (Bennett et al., 1991; Musil and Goodenough, 1991; Goodenough et al., 1996; Kumar and Gilula, 1996), it is still not known how junctional communication is regulated under physiological conditions. Regulation of cell–cell communication has often been evaluated by using nonphysiological effectors such as ionophores, phorbol esters, or cell-permeable cAMP analogues. There is evidence that an increase in cytoplasmic Ca^{2+} or H^+ levels can disrupt cell–cell coupling (Spray, 1994), whereas a rise in cAMP frequently upregulates junctional communication (Godwin et al., 1993; Burghardt et al., 1995; Goodenough et al., 1997; but see Lasater, 1987, for an opposite effect). Furthermore, membrane potential (transjunctional voltage) has been implicated in the gating of gap junction channels (for references see Beyer, 1993). Of particular relevance is the finding that several protein kinases can influence junctional permeability (for reviews see Hotz-Wagenblatt and Shalloway, 1993; Goodenough et al., 1996). For example, persistent activation of protein kinase C (PKC) or expression of the active v-Src tyrosine kinase abrogates cell–cell communication, which correlates with enhanced phosphorylation of Cx43 on serine or tyrosine residues, respectively (Crow et al., 1990; Filson et al., 1990). EGF inhibits junctional communication in some cell types (Maldonado et al., 1988) and stimulates serine phosphorylation of Cx43, which is thought to be mediated by mitogen-activated pro-

---

Jacqueline Alblas' current address is Department of Pulmonary Diseases, University Hospital Utrecht, 3584 CX Utrecht, The Netherlands.

Address all correspondence to Wouter H. Moolenaar, The Netherlands Cancer Institute, Division of Cellular Biochemistry, Plesmanlaan 121, 1066 CX Amsterdam, The Netherlands. Tel.: +31-20-512 1971. Fax: +31-20-512 1989. E-mail: wmoolen@nki.nl

1. *Abbreviations used in this paper*: Cx43, connexin43; Et, endothelin; LPA, lysophosphatidic acid; LY, Lucifer yellow; MAP, mitogen-activated protein; NKA, neurokinin A; PKC, protein kinase C; PTX, pertussis toxin; TRP, thrombin receptor–activating peptide.

This document was created with FrameMaker 4.0.4

tein (MAP) kinase (Kanemitsu and Lau, 1993; Hii et al., 1994). Consistent with this, MAP kinase can directly phosphorylate Cx43 in vitro (Warn-Cramer et al., 1996). However, no specific receptor-linked signaling pathway involved in modulating junctional communication has been identified to date.

Lysophosphatidic acid (LPA) is a platelet-derived serum mitogen that acts on its cognate G protein–coupled receptor present in numerous cell types (Moolenaar et al., 1997). The LPA receptor couples to stimulation of phospholipase C, inhibition of adenylyl cyclase, and activation of the Ras and Rho GTPases (Moolenaar et al., 1997). In a recent patch-clamp study on confluent Rat-1 fibroblasts, we found that LPA evokes a long-lasting membrane depolarization due to activation of a Cl^- conductance (Postma et al., 1996). While analyzing Cl^- channel opening in response to LPA, we made the unexpected observation that the cell under study rapidly isolates itself from adjacent cells. This prompted us to analyze G protein regulation of cell–cell communication in more detail. Rat-1 cells are ideally suited for these studies because (*a*) they express Cx43 as the sole gap junction protein (Goldberg and Lau, 1993) and (*b*) G protein signaling is well characterized in these cells (van Corven et al. 1989, 1993; Hordijk et al., 1994*a*; Postma et al., 1996; van Biesen et al., 1996; Kranenburg et al., 1997).

Using a newly developed single patch-clamp electrode technique together with dye coupling studies, we show here that Cx43-based junctional communication is rapidly but transiently disrupted upon activation of various G protein–coupled receptors, including those for LPA, thrombin, and neuropeptides. We show that agonist-induced gap junction closure is independent of Ca^{2+}, PKC, MAP kinase, membrane potential, and Ras/Rho signaling. Instead, we find that Cx43-based gap junctions are closed through a novel G protein–mediated signaling pathway involving c-Src. In addition, we show that recovery of communication is controlled, at least in part, by homologous receptor desensitization.

Materials and Methods

Materials

Staurosporine, tyrphostins 25 and 47, sodium orthovanadate, 8-Br-cAMP, and 8-Br-cGMP were from Calbiochem-Novabiochem (La Jolla, CA). Lucifer yellow (LY), Indo-1, and rhodamine-conjugated palloidin were from Molecular Probes (Eugene, OR). EGF was from Collaborative Research Inc. (Waltham, MA). LPA (1-oleoyl), thrombin, endothelin, neurokinin A, isoproterenol, phorbol ester, ionomycin, and thapsigargin were from Sigma Chemcial Co. (St. Louis, MO). TRP (sequence: SFLLRNPND-KYEPF) was synthesized as described (Jalink and Moolenaar, 1992). C3 and pertussis toxin were from List Laboratories. Antibodies to Cx43 and phosphotyrosine (PY20) were from Transduction Laboratories (Lexington, KY) and anti-Src monoclonal 327 from Oncogene Science (Manhasset, NY). [γ-^{32}P]ATP was from Amersham Corp. (Arlington, Heights, IL).

Cell Culture

Rat-1 cells, v-Src–transformed Rat-1 cells (B77 cells; van der Valk et al., 1987), Rat-1 cells expressing wild-type or truncated NK2 receptor (Alblas et al., 1995, 1996), HEK 293 cells, HeLa cells, and mouse embryonic fibroblasts, either expressing or lacking endogenous c-Src (kindly provided by P. Soriano [Fred Hutchinson Cancer Research Center, Seattle, WA] and K. Burridge [University of North Carolina, Chapel Hill, NC]), were grown in DME supplemented with 7.5% fetal calf serum and antibiotics. Cells were grown to confluency and then exposed to serum-free DME for 16–24 h.

Electrophysiology: Single Electrode Measurements

Electrophysiological recordings were obtained from cells grown in 3-cm culture dishes using the whole-cell patch-clamp technique as described (Postma et al., 1996). By analyzing current relaxations evoked by brief voltage steps, the degree of cell–cell coupling can be monitored continuously by a single patch-clamp electrode (see Results and Fig. 2), as opposed to the dual-electrode techniques used in most coupling studies (for single-electrode analysis of cell–cell coupling see also Bigiani and Roper, 1995). Data were collected using an EPC-7 amplifier (List-Medical, Darmstadt, Germany), interfaced to a personal computer via an A/D converter (TL-1 DMA interface; Axon Instruments, Inc., Foster City, CA). Voltage-clamp protocols were generated, and data were stored and analyzed using pClamp 6.0 (Axon Instruments, Inc.). Recordings were carried out using the perforated patch-clamp technique with amphotericin in the pipette solution (to selectively permeabilize the membrane to monovalent ions; Rae et al., 1991; Postma et al., 1996). Micropipettes were fire-polished and filled with a high K^+, low Ca^{2+} buffer as described (Postma et al., 1996). Capacitive transients caused by the patch-pipette were compensated for. Agonists and pharmacological agents were applied either from a pipette positioned close to the cell(s) under study or by bath perfusion. Capacitive current transients were fitted using the Chebyshev method. Based on a a minimal electrical equivalent circuit (Lindau and Neher, 1988), the current transient recorded from non-coupled cells was fitted with a single decay time constant (one exponential). However, the transient from coupled cells in a monolayer is considerably more complex; in first approximation, it can be fitted by two exponentials with time constants τ_1 and τ_2 (see Results and Fig. 2; see also Bigiani and Roper, 1995, for the case of a coupled cell pair). The first exponential component largely reflects the charging of the patched cell, and the second component that of the coupled cells. This is further illustrated in the model experiment of Fig. 2. Changes in junctional conductance manifest themselves as changes in time constants and steady-state currents; however, unlike the case of just two coupled cells (Bigiani and Roper, 1995), junctional conductance in a coupled monolayer cannot readily be calculated from the capacitive transients and steady-state currents measured. All experiments were done at least in triplicate; results are given as means ± SEM and statistical significance was established using Student's *t* test.

LY Diffusion

Gap junction permeability was determined using both the LY scrape-loading technique (El-Fouly et al., 1987) and the LY microinjection method. For scrape-loading, confluent cells in 3-cm dishes were stimulated with agonist for various periods of time. A scrape line was made on the monolayer using a surgical blade in medium containing 5 mM LY. LY was allowed to diffuse for 5 min. Immediately thereafter, the cultures were washed with PBS, fixed in 3.7% paraformaldehyde, and treated with antibleach reagent (Vectashield). Quantitative analysis of LY diffusion was carried out with a confocal microscope coupled to an image analyzer system (Bio-Rad Laboratories, Hercules, CA), measuring the average pixel intensity in the direction parallel to the scrape line as a function of diffusion distance.

In a separate series of experiments, we monitored LY diffusion from a single microinjected Rat-1 cell within a monolayer. Cells were treated with agonist for 5 min and then microinjected with a mixture of LY (100 μM) and ethidium bromide (0.5 mg/ml; for nuclear staining). After microinjection, cells were washed with PBS, and intracellular LY/ethidium bromide fluorescence was monitored immediately thereafter (total LY diffusion time: 2 min).

cDNA Transfection

Rat-1 cells stably transfected with wild-type or truncated NK2 receptor have been described recently (Alblas et al., 1995, 1996). For stable transfection of dominant-negative Src into NK2-receptor–expressing Rat-1 cells, 10 μg of pMT2-plasmid containing the complete cDNA of kinase-inactive Src (SrcK$^-$; mutation Lys295Met; cDNA provided by S. Courtneidge, Sugen, Inc., Redwood City, CA) together with 0.2 μg of pDH containing the hygromycin resistance gene was transfected using standard calcium phosphate precipitation. After 16 h, cells were split 1:10 and then exposed to selection medium containing 200 U/ml hygromycin. Hygromy-

cin-resistant clones were isolated and screened for enhanced Src protein expression in immunoblots using anti-Src monoclonal antibody 327.

Immunoblotting and Cx43 Immunoprecipitations

For immunoblotting, confluent cells were treated with agonist for various periods of time, washed with ice-cold PBS, and lysed in SDS-sample buffer. Proteins were subjected to SDS-PAGE and transferred to nitrocellulose. The filters were blocked with 3% BSA in TBST (10 mM Tris, pH 8.0, 150 mM NaCl, 0.05% Tween 20) and incubated with antibody for 1 h. After washing with TBST, blots were incubated with peroxidase-conjugated rabbit anti–mouse Ig, washed again, and subjected to the ECL procedure. For immunoprecipitation of Cx43, cells were lysed in NP-40 lysis buffer (50 mM Tris-HCl, pH 7.4, 1% NP-40, 0.25 mM Na-deoxycholate, 150 mM NaCl, 2 mM EGTA, 0.1 mM Na_3VO_4, 10 mM NaF, 0.1 mM PMSF fluoride, 10 mg/ml leupeptin, 10 mg/ml aprotinin). Cell lysates were immunoprecipitated with anti-Cx43 antibody. Precipitated proteins were resolved by SDS-PAGE on 12.5% polyacrylamide gels and either processed for ECL visualization or transferred to nitrocellulose for immunoblotting (see above).

Fluorescence Microscopy

Cells were grown on glass coverslips, fixed in PBS containing 4% paraformaldehyde, and incubated with either anti-Cx43 antibody followed by fluorescent staining using FITC-conjugated rabbit anti–mouse Ig. For F-actin staining, fixed cells were incubated with rhodamine-conjugated phalloidin. Fluorescence was visualized using confocal microscopy.

Src Kinase Assay

Cells were stimulated with agonists for various periods of time, washed with ice-cold PBS, and solubilized in 0.5 ml of lysis buffer (25 mM Tris pH 7.4, 0.5% NP-40, 150 mM NaCl, 1 mM DTT, 0.1 mM Na_3VO_4, 10 mM $Na_2P_2O_4$, 10 mM NaF, 0.1 mM PMSF fluoride, 10 µg/ml leupeptin, 10 µg/ml aprotinin) on ice for 10 min. Lysates were precleared twice with normal mouse serum precoupled to Sepharose–protein A beads (30 min, 4°C). Src was immunoprecipitated with monoclonal 327 (1 h, 4°C). The precipitates were washed four times with lysis buffer and washed once with ATP-free kinase buffer (20 mM Hepes, pH 7.4, 10 mM $MgCl_2$, 1 mM DTT). In vitro kinase assays were carried out in 30 ml of kinase buffer supplemented with 0.25 mg/ml enolase, 20 µM ATP and 0.5 mCi/ml [γ-^{32}P]ATP for 10 min on ice. The reactions were stopped by addition of SDS-sample buffer; the samples were then boiled and analyzed by SDS-PAGE (10% polyacrylamide). After autoradiography, the amount of ^{32}P present in Src and enolase was determined by PhosphoImager analysis.

Results

Rapid Changes in Cell–Cell Communication Monitored with a Single Patch-Clamp Electrode

We recently showed that LPA, like serum, rapidly activates a depolarizing Cl^- current in confluent Rat-1 fibroblasts (Postma et al., 1996). Surprisingly, activation of this current is accompanied by a dramatic (~40-fold) fall in cell input conductance, monitored as the current response to brief voltage pulses (Fig. 1, A and B). This conductance decrease develops rapidly and is maximal after a few minutes (Fig. 1 B). It thus appears that LPA-induced opening of Cl^- channels is overridden by the simultaneous closure of other channels. Since confluent fibroblasts are electrically coupled (through Cx43) and thus behave as if the monolayer were one large cell, the overall input conductance is determined by both transmembrane and cell-to-cell conductances. Given the finding that LPA increases transmembrane conductance (Cl^--selective), the observed fall in input conductance must result from a concomitant closure of gap junction channels.

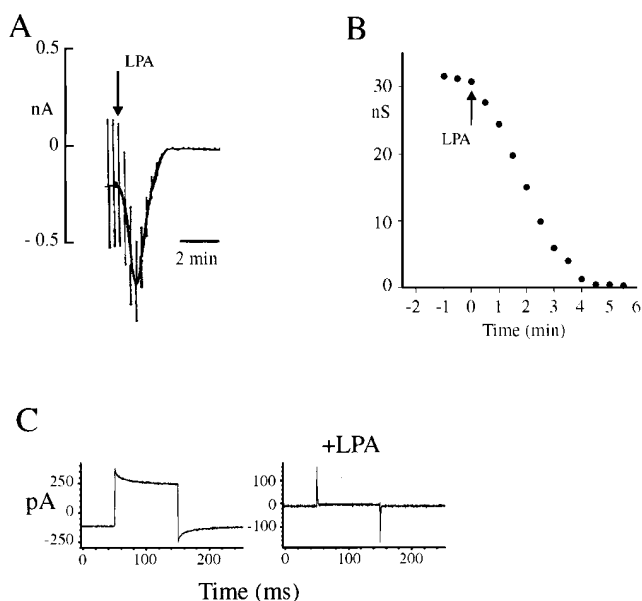Direct support for this notion comes from analysis of the

Figure 1. Modulation of cell–cell coupling measured by a single patch-clamp electrode. (A) Whole-cell current and input resistance measurements in LPA-stimulated Rat-1 cells in monolayer. Input resistance was measured as the current response to alternating voltage steps (10 mV; duration 400 ms; holding potential −60 mV). It is seen that LPA induces a transient inward current (carried by Cl^-; Postma et al., 1996) accompanied by a long-lasting increase in input resistance due to LPA-induced inhibition of electrical cell–cell coupling (see text and Fig. 2 A). (B) Time course of LPA-induced fall in input conductance, reflecting inhibition of cell–cell coupling (see text and Fig. 2 A). LPA (1 µM) was added at time zero. Data points were calculated from the current deflections in Fig. 1 A. (C) Capacitive current transients evoked by a 10-mV voltage pulse (duration 100 ms; holding potential −70 mV) recorded from confluent Rat-1 cells, before and 5 min after addition of LPA (1 µM) as indicated. Double exponential fits are superimposed on the current traces (see Materials and Methods).

typical current relaxations in response to a voltage step before and immediately after LPA addition (Fig. 1 C). This current response consists of an initial capacitive transient decaying to a steady-state value. It is seen that LPA reduces not only the amplitude of the steady-state current but also the decay time constant(s) of the capacitive transient (Fig. 1 C). These complex changes in electrical properties of the monolayer can only be explained by acute loss of electrical cell–cell coupling. This is exemplified in a model experiment, illustrated in Fig. 2 A, which shows the different current responses recorded from an increasing number of coupled cells. Time constant and steady-state currents are seen to increase with increasing number of contacting adjacent cells, as detailed in the legend to Fig. 2 A. Fig. 2 B shows that the current response of a single isolated cell is hardly affected by LPA. This demonstrates that the observed electrophysiological changes in LPA-treated monolayers (Fig. 1 C) result from altered cell–cell coupling, not from altered membrane conductance. Thus, by analyzing current relaxations in response to brief voltage steps, the degree of cell–cell coupling can be monitored continuously by a single patch-clamp electrode, as opposed to the dual-electrode techniques used in most
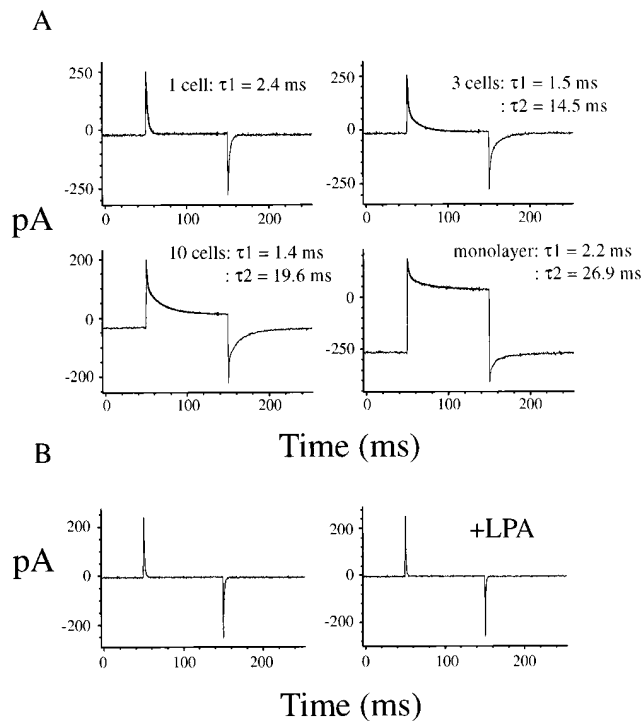
A

1 cell: τ1 = 2.4 ms

3 cells: τ1 = 1.5 ms
    : τ2 = 14.5 ms

10 cells: τ1 = 1.4 ms
     : τ2 = 19.6 ms

monolayer: τ1 = 2.2 ms
       : τ2 = 26.9 ms

pA

Time (ms)

B

pA

+LPA

Time (ms)

Figure 2. (*A*) Whole-cell current responses to a 10-mV voltage pulse (duration 100 ms; holding potential −70 mV) recorded from different cell configurations as indicated. In the case of a single cell, the capacitive transient can be fitted and characterized by one decay time constant τ. Time constant and steady-state currents are seen to increase with increasing number of contacting adjacent cells. A minimal equivalent electrical circuit in which the capacitive current response of the cell under the patch-pipette is represented by one time constant (τ_1) and that of the contacting neighbors by a second (τ_2). With increasing number of coupled cells, τ_2 increases whereas τ_1 remains virtually unaltered. Steady-state currents increase with increasing cell population size because of a proportional decrease in overall input resistance. Curve fitting gave the τ values indicated. (*B*) Current response to a 10-mV voltage pulse, as in *A*, recorded from a single, isolated cell before and after LPA treatment (1 μM; 5 min).
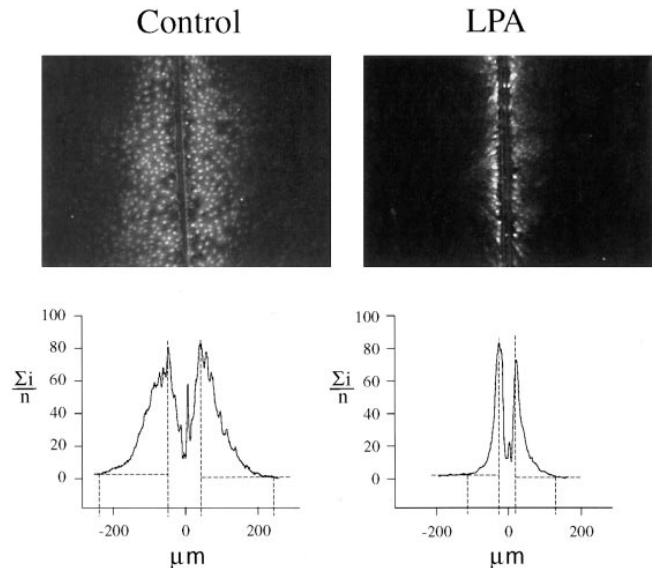
Control   LPA

Figure 3. Inhibition of LY transfer. LY was scrape-loaded into confluent Rat-1 cells and cell-to-cell diffusion followed for 5 min in both control and LPA-treated cells as indicated. LY diffusion distance (μm) was quantitated by calculating the average fluorescence intensities as a function of distance from the scrape line. $\Sigma i/n$ (y-axis) denotes average pixel intensity (*i*, pixel intensity; *n*, number of pixels). The difference in distance between peak intensities and the point where LY fluorescence equals background is a measure of junctional permeability. When corrected for "background" fluorescence (resulting from scrape damage), LPA treatment reduced the basal lateral LY diffusion distance from 361 ± 9 μm (*n* = 108) to 158 ± 8 μm (*n* = 60).

coupling studies. Single-electrode analysis of cell–cell coupling (between two cells) has also been documented by Bigiani and Roper (1995).

The electrophysiological studies were complemented by LY diffusion experiments, in which we determined the cell-to-cell diffusion distance of intracellularly loaded LY per unit time period. Fig. 3 shows a typical LY scrape-loading experiment revealing that cell-to-cell LY transfer in confluent Rat-1 cells is markedly inhibited by LPA. The results obtained from the LY scrape-loading experiments were supported by microinjection studies, in which we monitored LY diffusion from single cells microinjected with LY (together with ethidium bromide) before and after agonist stimulation (Fig. 4). Under control conditions, LY diffusion from the microinjected cell was very rapid: at 2 min after microinjection, LY fluorescence was detectable in 64 ± 6 surrounding cells (means ± SEM; number of dishes *n* = 17). After stimulation for 5 min with LPA (1 μM), intercellular LY diffusion was detectable in only

10 ± 3 (*n* = 11) surrounding cells. Rapid inhibition of cell–cell coupling was not unique for LPA (see below). Strongest inhibition of LY diffusion was observed with the G protein–coupled receptor agonist endothelin, which completely blocked LY diffusion from the microinjected cell in all dishes tested (*n* = 13; Fig. 4; see also Fig. 5, *B* and *C*, for electrophysiological and LY scrape-loading data). In all these experiments, the transmembrane permeability to LY was not affected by agonist stimulation, as both stimulated and control cells showed negligible dye loss over a 15-min period. Thus, the observed inhibition of LY diffusion represents an agonist-induced decrease in gap junction permeability.

Loss of Communication Is Induced by a Variety of G protein–coupled Receptors

We tested a number of agents and agonists for their ability to inhibit cell–cell communication. Uncoupling was also induced by AlF_4^-, a direct activator of trimeric G proteins (Kahn, 1991), consistent with LPA action being G protein mediated (Fig. 5 *A*). Its inhibitory effect develops rather slowly, consistent with a lag required for AlF_4^- entry into the cells.

In addition to LPA, the G protein–coupled receptor agonists endothelin, thrombin as well as a thrombin receptor agonist peptide (TRP; Jalink and Moolenaar, 1992) all rapidly inhibit cell–cell coupling in Rat-1 cells, as revealed by both electrophysiological and LY transfer experiments
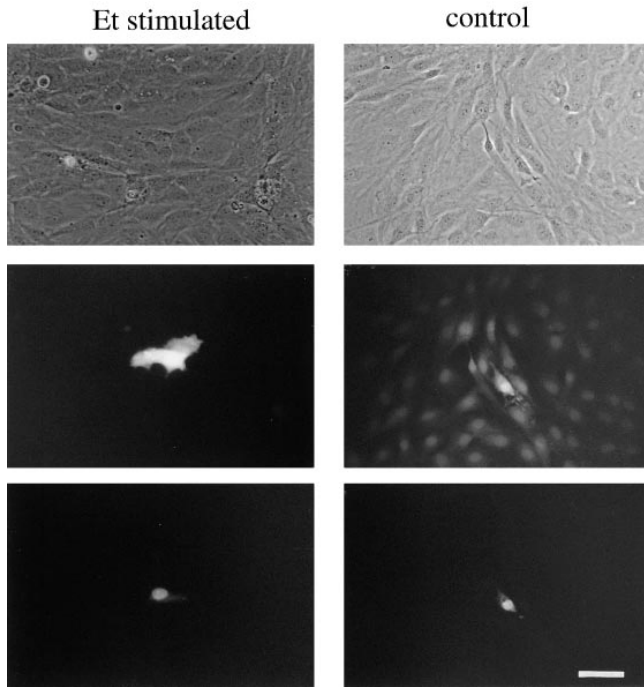
Et stimulated   control

Figure 4. LY diffusion from a microinjected cell. LY was pressure-injected together with ethidium bromide into a single Rat-1 cell in a monolayer. LY diffusion into adjacent cells was monitored over a 2-min time period before and after stimulation with endothelin (50 nM). (*Top*) Phase-contrast micrographs. (*Middle*) LY fluorescence. (*Bottom*) Ethidium bromide staining indicating microinjected cell. At 2 min after microinjection, LY fluorescence was detectable in 64 ± 6 surrounding cells (means $\pm$ SEM; number of dishes $n = 17$). Endothelin stimulation consistently resulted in complete loss of LY diffusion ($n = 13$). After stimulation for 5 min with LPA (1 μM), intercellular LY diffusion was detectable in 10 ± 3 ($n = 11$) surrounding cells. Bar, 50 μm.

and summarized in Fig. 5, *B* and *C* (see also Fig. 4). Of note, these agonists also mimic LPA in evoking a depolarizing Cl$^-$ current in Rat-1 cells (Postma et al., 1996). Pretreatment of the cells with pertussis toxin (PTX) did not

---

Figure 5. Loss of cell–cell coupling caused by a variety of G protein–coupled receptors. (*A*) Inhibitory effect of AlF$_4^-$ on junctional conductance. Decrease in junctional conductance was measured as a decrease in input conductance monitored as the current response to alternating voltage steps as in Fig. 1 *A*. (*B*) Modulation of junctional conductance by various stimuli, as revealed by changes in decay time constant (τ, ms) and steady-state input conductance (*g*, μSiemens). Values represent averaged data derived from exponential fits of current responses to 10-mV voltage pulses (as in Fig. 1, *A* and *C*), measured at 10 min after agonist addition. Final concentrations (*n*, number of experiments): EGF, 50 ng/ml ($n = 19$); AlF$_4^-$, 10 μM ($n = 3$); LPA, 1 μM ($n = 21$); TRP, 100 μM ($n = 9$); ET (endothelin), 50 nM ($n = 4$); NKA, 1 μM ($n = 14$). *C*, nonstimulated control cells ($n = 47$). Values represent means $\pm$ SEM. (*C*) Inhibition of LY diffusion (measured by the scrape-loading assay) induced by the indicated agonists and pharmacological agents. Final concentrations (*n*, number of experiments): Et (endothelin), 50 nM ($n = 61$); PTX, 100 ng/ml ($n = 10$; 24-h pretreatment); TPA (100 nM) treatment for 24 h ($n = 10$) or 10 min ($n = 12$); LPA, 1 μM ($n = 60$); EGF, 50 ng/ml ($n = 12$). Values represent means $\pm$ SEM and are corrected
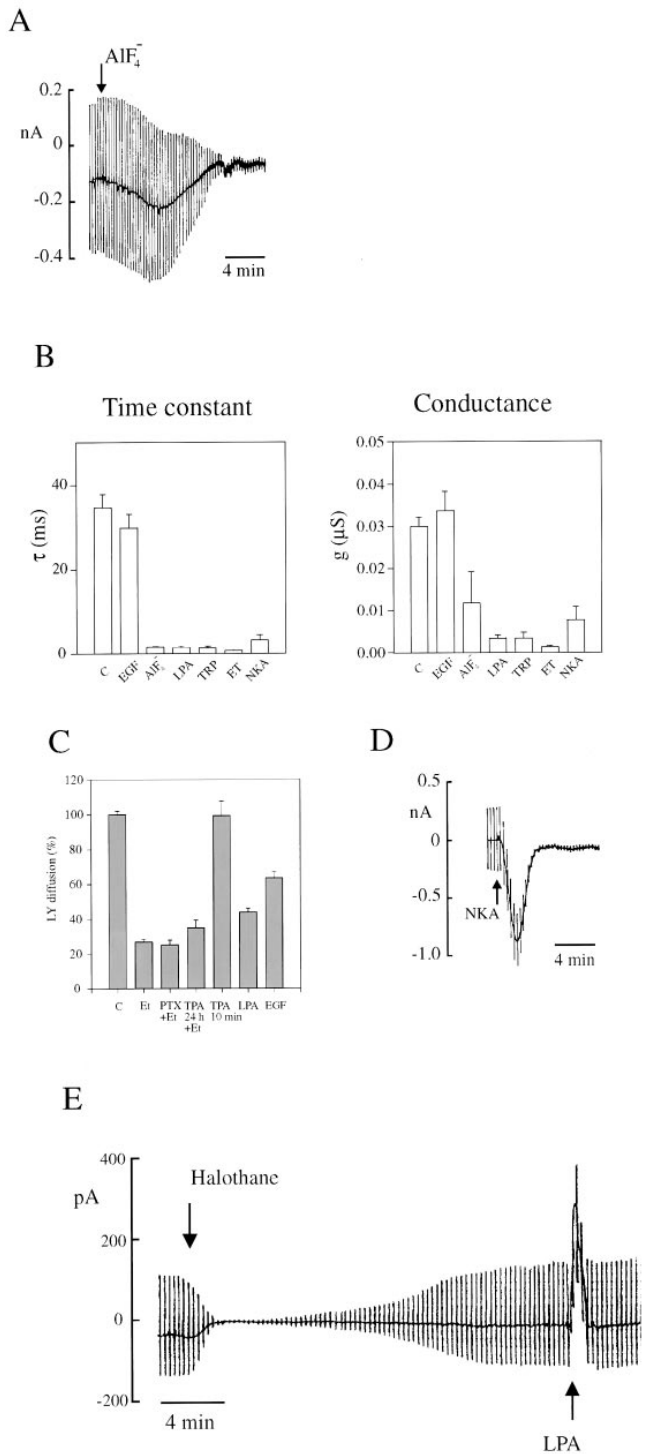
for background fluorescence resulting from scrape damage. (*D*) Voltage-clamp recording from confluent Rat-1 cells expressing the human NK2 receptor for NKA (Alblas et al., 1995). Input resistance was measured as in Fig. 1 *A*. As with LPA (Fig. 1 *A*), NKA (1 μM) activates an inward Cl$^-$ current accompanied by a dramatic fall in input conductance. (*E*) Lack of inhibitory effect of LPA in HeLa cells. Halothane (0.5%) was used as a positive control. It is seen that cell–cell coupling is acutely disrupted by halothane followed by its gradual recovery upon spontaneous evaporation of halothane from the dish. LPA evokes a transient outward K$^+$ current (Ca^{2+}-dependent), without affecting electrical cell–cell coupling.

Control   Et
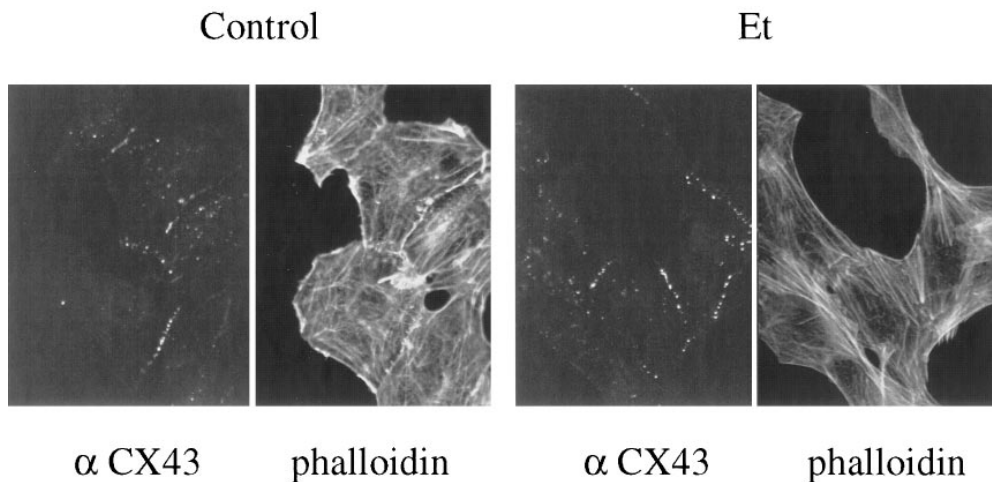
α CX43   phalloidin   α CX43   phalloidin

Figure 6. Localization of Cx43 in Rat-1 cell monolayers. Immunofluorescence of Cx43 in both nonstimulated control cells and cells treated with Et (50 nM) for 10 min. Cells were also stained for F-actin using rhodamine-conjugated phalloidin. Note characteristic punctate Cx43 staining at cell–cell contacts, which remains unaltered after endothelin treatment, and endothelin-induced formation of actin stress fibers.

affect agonist action, indicating that G_i proteins are not involved (Fig. 5 *C*). Activation of endogenous β-adrenergic receptors by isoproterenol, which raises cAMP in Rat-1 cells (van Corven et al., 1989), left cell–cell coupling unaltered. EGF, a potent mitogen for Rat-1 cells (van Corven et al., 1989), failed to inhibit electrical coupling, although intercellular LY diffusion was somewhat reduced (Fig. 5 *C* and results not shown). This would suggest that EGF may decrease junctional permeability to larger molecules only, but further experiments are required to test this hypothesis.

Thus, inhibition of cell–cell communication is a common response to a subclass of G protein–coupled receptors, notably those that couple to PTX-insensitive G proteins ($G_{q/11}$ and $G_{12/13}$ subfamily). Support for this notion comes from transfection studies using the human NK-2 receptor for neurokinin A (NKA; or substance K). When stably expressed in Rat-1 cells, the NK-2 receptor couples to G_q-mediated inositol lipid breakdown and Ca^{2+} mobilization (Alblas et al., 1995, 1996). Ligand stimulation of the transfected NK2 receptor triggers rapid gap junction closure (Fig. 5, *B* and *D*) with concomitant activation of the inward Cl^- current (Postma et al., 1996).

Involvement of Cx43

Cx43 is the only gap junction protein thus far identified in fibroblasts (Goldberg and Lau, 1993). Fig. 6 shows the characteristic punctate staining of Cx43 at sites of cell–cell contact. Endothelin treatment does not detectably alter the localization pattern of Cx43 over a 10-min time period (Fig. 6) nor the levels of endogenous Cx43 (as determined by Western blotting; see below).

The inhibitory effect of LPA on cell–cell communication was also observed in Cx43-expressing epithelial cells (HEK 293 cells; results not shown). In contrast, no effect of LPA on junctional conductance was observed in Cx43-deficient HeLa cells, which are electrically coupled (albeit weakly; see also Eckert et al., 1993) and do express functional LPA receptors (Jalink et al., 1995). Fig. 5 *E* shows that, while junctional communication in HeLa cells is rapidly blocked by the general anesthetic halothane, LPA only induces a transient outward current in these cells without any sign of decreased cell–cell coupling. Taken to-

gether, these results are consistent with Cx43 being the primary target of agonist action.

Recovery of Communication: Regulation by Receptor Desensitization

After the acute loss of communication in response to agonists, cell coupling recovers gradually over time. In the continuous presence of LPA, TRP, or NKA, recovery of communication was usually complete within 1–2 h (Fig. 7); in endothelin-stimulated cells, full recovery took somewhat longer (3–4 h; not shown).

How are the kinetics of this recovery regulated? One possibility is that recovery is due to receptor-mediated signal attenuation ("desensitization"). To examine this point, we used a mutant NK2 receptor in which the COOH-terminal "desensitization domain" (70 residues) is deleted (Alblas et al., 1995). When expressed in Rat-1 cells, such desensitization-defective receptors mediate prolonged inositol lipid breakdown and sustained MAP kinase activation, as opposed to the short-lived responses induced by wild-type receptors; furthermore, the liganded mutant receptor induces both DNA synthesis and morphological transformation in response to ligand, whereas wild-type receptor does not (Alblas et al., 1995, 1996).

When Rat-1 cells expressing mutant NK2 receptor were exposed to ligand, the cells remained uncoupled for a much longer time period than observed with wild-type receptors (Fig. 7, *bottom*). Cell–cell coupling had returned to control values only after ~12 h. These results indicate that recovery of communication is regulated by receptor desensitization and, furthermore, that there is a correlation between the duration of receptor-mediated gap junction closure and subsequent morphological transformation (Alblas et al., 1996).

Dissection of Signaling Pathways

Which G protein–effector pathways may underlie inhibition of cell–cell communication? Since agonist-induced gap junction closure is resistant to PTX (Fig. 5 *C*), which blocks LPA- and thrombin-induced Ras-GTP accumulation and MAP kinase activation in Rat-1 cells (van Corven
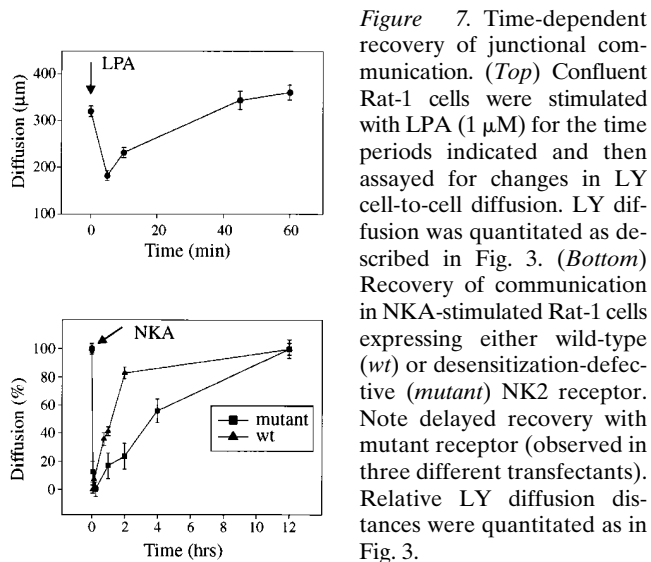
Figure 7. Time-dependent recovery of junctional communication. (*Top*) Confluent Rat-1 cells were stimulated with LPA (1 µM) for the time periods indicated and then assayed for changes in LY cell-to-cell diffusion. LY diffusion was quantitated as described in Fig. 3. (*Bottom*) Recovery of communication in NKA-stimulated Rat-1 cells expressing either wild-type (*wt*) or desensitization-defective (*mutant*) NK2 receptor. Note delayed recovery with mutant receptor (observed in three different transfectants). Relative LY diffusion distances were quantitated as in Fig. 3.

Figure 8. Agonist-induced Ca^{2+} signaling and Rho activation are not required for gap junction closure. (*A*) Top traces represent typical Ca^{2+} recordings from Indo-1–loaded Rat-1 cells on a glass coverslip. For experimental details see Jalink and Moolenaar (1992). Arrows indicate time of addition of agonist or reagent. Concentrations used: LPA, 1 µM; EGTA, 3 mM; ionomycin, 2.5 µM; TRP, 100µM; Et, 1 µM. Bottom traces are from parallel electrophysiological experiments in Ca^{2+}-depleted cells (treated with EGTA and ionomycin as above). Medium contained 100 µM $LaCl_3$ to allow proper pipette sealing in Ca^{2+}-free medium and to block residual transmembrane Ca^{2+} fluxes. Electrophysiological details as in Fig. 1. Agonist-induced fall in junctional conductance is seen to be independent of Ca^{2+} signaling. (*B*) Patch-clamp recording in cells pretreated for 18 h with Rho-inactivating C3 toxin (30 µg/ml). Note that C3 treatment does not affect agonist (Et)-induced electrophysiological responses, including the fall in junctional conductance, whereas formation of actin stress fibers is fully inhibited (photographs). Photographs show F-actin staining in the same cells stimulated with Et before (*upper*) and after (*lower*) C3 treatment. F-actin staining was done as described in Alblas et al. (1996).

et al., 1993; Hordijk et al., 1994*a*; Kranenburg et al., 1997), it follows that gap junction closure is independent of Ras-MAP kinase signaling. Consistent with this, treatment of Rat-1 cells with 8Br-cAMP (1 mM) did not affect LPA-induced gap junction closure (not shown), whereas MAP kinase activation is completely blocked by 8Br-cAMP (Hordijk et al., 1994*b*).

Strikingly, the G protein–coupled receptors that mediate gap junction closure all couple to inositol lipid breakdown and consequent Ca^{2+} mobilization in Rat-1 cells. However, gap junctions did not close in response to ionomycin (25 nM), which raises cytosolic $[Ca^{2+}]$ to micromolar levels (Postma et al., 1996). Conversely, agonist-induced gap junction closure was not impaired when cells were depleted of intracellular free Ca^{2+} by addition of ionomycin in Ca^{2+}-free, La^{3+}-containing medium or by preincubation with 200 nM thapsigargin (Fig. 8 *A*, and results not shown). Furthermore, gap junctions did not close in response to PKC-activating phorbol ester (TPA; 100 nM), as shown in Fig. 5 *C*. Prolonged (24 h) pretreatment of the cells with TPA (1 µM; 24 h) to downregulate PKC did not prevent cell uncoupling (Fig. 5 *C*), nor did the PKC inhibitor Ro-31-8220 (5 µM) have any effect. These results contrast with reports that show marked inhibitory effects of phorbol ester on junctional communication in some cell types (for review see Goodenough et al., 1996). Taken together, our results indicate that activation of the Ca^{2+}-PKC pathway is neither necessary nor sufficient for gap junction closure in Rat-1 cells.

Agonist-induced uncoupling also correlates with Cl^--mediated membrane depolarization (Postma et al., 1996). However, artificial membrane depolarization, induced either by altering the holding potential or by exposing the cells to high $[K^+]$, had no detectable effect on cell coupling nor on the response to agonists. Thus, gap junction closure is not secondary to membrane depolarization.

LPA, thrombin, endothelin and NKA also rapidly activate the Ras-related Rho GTPase, leading to the formation of actin stress fibers, which is a PTX-insensitive process (Ridley and Hall, 1992; Alblas et al., 1996; Postma et al.,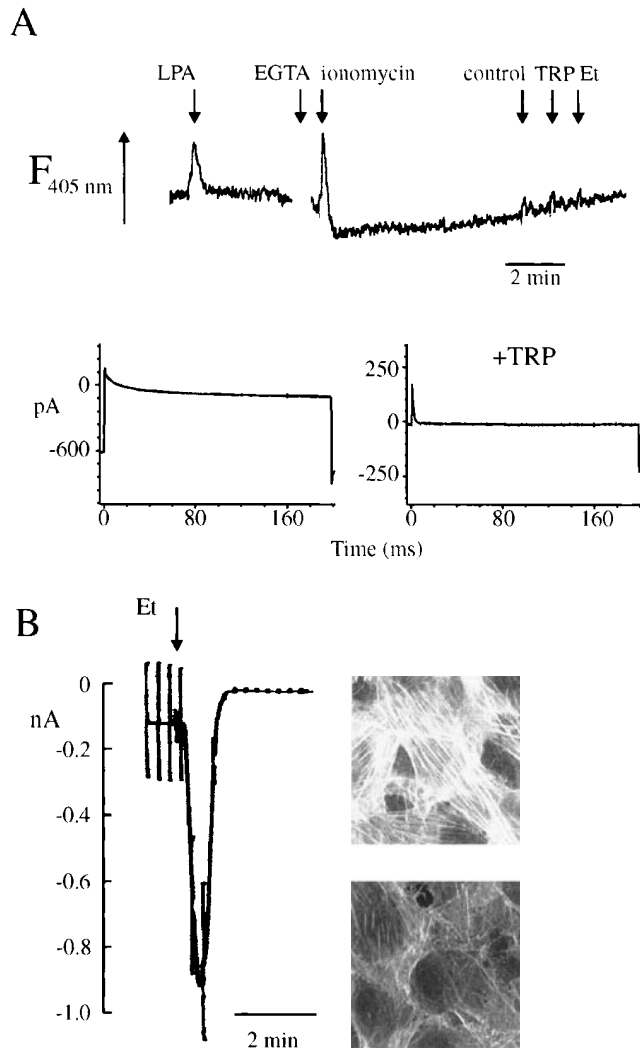 1996). The bacterial C3 toxin, which modifies and thereby inactivates Rho (Machesky and Hall, 1996), did not affect agonist-induced gap junction closure under conditions where stress fiber formation was fully inhibited (Fig. 8 *B*). This indicates that gap junction closure is independent of Rho signaling.
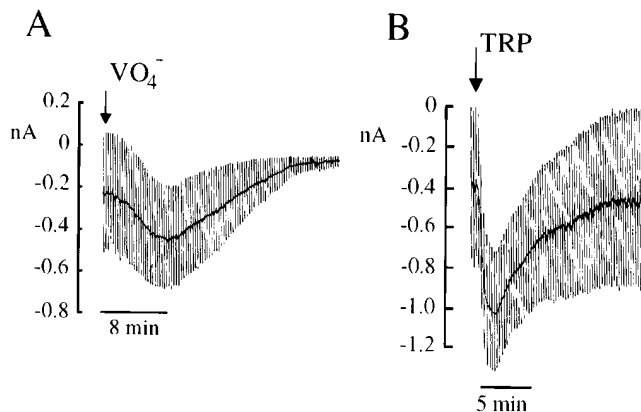
Figure 9. Tyrosine phosphorylation and loss of Cx43-based cell–cell communication. (*A*) The tyrosine phosphatase inhibitor pervanadate inhibits junctional conductance. Alternating voltage steps were generated (400 ms, 10 mV) from holding potential (-60 mV) to monitor input conductance. Inhibition of junctional conductance by pervanadate is accompanied by tyrosine phosphorylation of Cx43 (see Fig. 11 *A*). Concentrations used: vanadate, 0.4 mM; H_2O_2, 4.8×10^{-4}% (140 nM). (*B*) Whole-cell current and conductance measurements in Rat-1 cells pretreated for 15 min with the tyrosine kinase inhibitor tyrphostin 25 (100 μM) and then stimulated with TRP (100 μM). Tyrphostin pretreatment is seen to prevent agonist-induced loss of cell–cell coupling but not activation of the inward Cl^- current. Similar results were obtained with tyrphostin 47 and other receptor agonists (LPA, NKA).

Tyrosine Kinase Involvement

We next examined the effects of tyrosine kinase and phosphatase inhibitors. Ortho-vanadate in conjunction with H_2O_2 (pervanadate) inhibits tyrosine phosphatases in vivo. Fig. 9 *A* shows that pervanadate treatment mimics agonist stimulation in causing complete inhibition of cell–cell communication in Rat-1 cells, albeit with slower kinetics, consistent with a lag required for vanadate entry into the cells.

Conversely, agonist-induced gap junction closure is fully prevented by the tyrosine kinase inhibitors tyrphostin 25 and 47 (Fig. 9 *B*). In contrast, the Ser/Thr kinase inhibitor staurosporine (100 nM) has no effect (not shown). The tyrphostins act selectively in that they do not affect activation of the inward Cl^- current (Fig. 9 *B*; Postma et al., 1996). These results suggest that G protein–mediated gap junction closure is regulated by a tyrosine kinase pathway.

Involvement of c-Src

Src family tyrosine kinases are attractive candidates for mediating gap junction closure since expression of active v-Src (or overexpression of c-Src) in 3T3 cells reduces junctional communication (Atkinson et al., 1981; Azarnia et al., 1988, 1989; Crow et al., 1990; Filson et al., 1990). We found that in v-Src–expressing Rat-1 cells (van der Valk et al., 1987), cell–cell communication is almost completely inhibited, while the expression and cell surface distribution of Cx43 is similar, at least qualitatively, to that in normal Rat-1 cells (not shown). If endogenous Src regulates G protein–mediated gap junction closure, then the agonists used should rapidly activate c-Src. Indeed, LPA, thrombin, and neuropeptides rapidly activate c-Src in Rat-1 cells and other fibroblasts (Chen et al., 1994; Rodriguez-Fernandez

and Rozengurt, 1996; van Biesen et al., 1996; Kranenburg et al., 1997). In addition, a rapid transient increase in c-Src activity is observed in response to NKA acting on the transfected NK2 receptor in Rat-1 cells; although the response is relatively small, it is statistically significant (Fig. 10 *A*).

To examine whether c-Src is required for inhibition of communication, we stably transfected Rat-1 cells with a kinase-inactive form of c-Src (SrcK$^-$). This Src mutant, in which the ATP binding site is inactivated (K295M mutation; Roche et al., 1995), should act in a dominant-negative manner by binding to proteins that interact with activated Src family members. Fibroblasts expressing SrcK$^-$ are viable but show a somewhat reduced growth rate (not shown; see also Broome and Hunter, 1996). When compared with control cells, SrcK$^-$-expressing cells exhibit similar basal tyrosine phosphorylation patterns, whereas ligand-induced tyrosine phosphorylation of cellular proteins (Hordijk et al. 1994*a*) is reduced (Fig. 10 *B*). When analyzed electrophysiologically, SrcK$^-$ cells showed normal cell–cell coupling. However, they failed to close their gap junctions in response to receptor stimulation, as shown in Fig. 10 *C*. It is also seen that gap junctions in SrcK$^-$ cells could still be closed (in a reversible manner) by the general anesthetic halothane. We note that expression of SrcK$^-$ does not interfere with activation of the inward Cl^- current (Fig. 10 *C*). Furthermore, we tested fibroblasts derived from Src$-/-$ mice (Bockholt and Burridge, 1995). In these Src-deficient cells, LPA, thrombin, and endothelin failed to inhibit gap junctional communication, whereas control cells showed a normal response, as shown in Fig. 10 *D*. However, the Src-deficient cells showed no anomalies in LPA-induced inward currents (not shown) or MAP kinase activation (Kranenburg et al., 1997). Taken together, these results indicate that c-Src is required for agonist-induced gap junction closure.

Having established a key role for c-Src in G protein–mediated gap junction closure, we examined the tyrosine phosphorylation state of Cx43 in Rat-1 cells under various conditions. First, we found that vanadate-induced gap junction closure is paralleled by prominent tyrosine phosphorylation of Cx43 (Fig. 11 *A*). Second, inhibition of junctional communication after v-Src expression is similarly associated with tyrosine phosphorylation of Cx43 (Fig. 11 *B*). However, our efforts to detect Cx43 tyrosine phosphorylation in response to LPA, TRP, or endothelin were unsuccessful under the conditions used.

Discussion

There has been much progress recently in understanding the biosynthesis and structure of connexin-based gap junction channels, their role in embryonic development and excitable tissue function, as well as their relationship to certain human diseases (Bennett et al., 1991; Beyer, 1993; Musil, 1994; Paul, 1995; Goodenough et al., 1996). One major unresolved question in the gap junction field is how junctional communication is regulated by physiological agonists. Although it has long been recognized that junctional conductance and permeability can be modulated by certain extracellular stimuli, relatively little progress has been made in identifying receptor-linked signaling pathways that modulate connexin function.
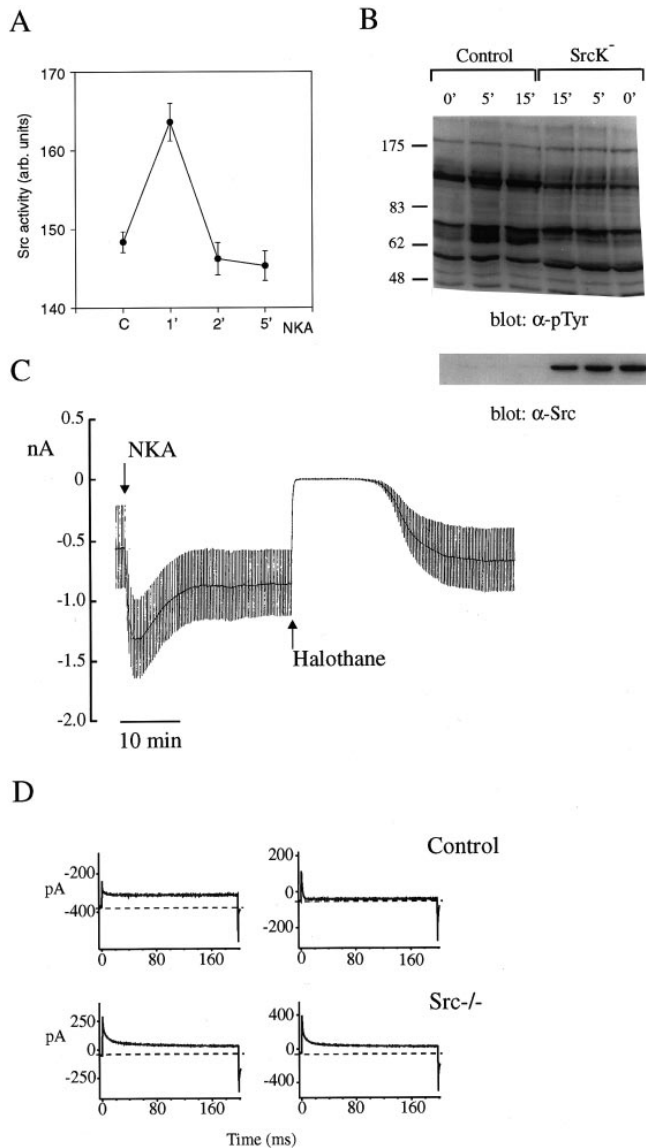
Figure 10. Involvement of Src. (*A*) Agonist-induced activation of c-Src. Serum-starved Rat-1 cells expressing the NK2 receptor were stimulated with NKA (1 μM) for the indicated times and then lysed. Endogenous c-Src was immunoprecipitated and assayed for kinase activity as described in Materials and Methods. The results represent the relative amount of ^{32}P incorporated in enolase, given as means ± SEM (arbitrary PhosphoImager units; triplicate determinations). (*B*) Overexpression of dominant-negative c-Src (SrcK$^-$) prevents gap junction closure. *Top*, NKA-induced tyrosine phosphorylation of cellular proteins in control cells and SrcK$^-$-transfected cells (dn-Src) expressing human NK2 receptor. Cells were stimulated with NKA (1 μM) for the indicated times and then lysed in SDS-sample buffer. Tyrosine-phosphorylated proteins were visualized using antiphosphotyrosine antibody PY20. Molecular mass markers (kD) are indicated on the left. Note reduction in agonist-induced protein tyrosine phosphorylations in the SrcK$^-$ cells when compared with control cells. *Bottom*, Western blot detection of Src using anti-Src antibody. (*C*) Current and conductance measurements in confluent Rat-1 cells expressing dominant-negative c-Src and NK2 receptor. Expression of dominant-negative Src prevents NKA-induced loss of cell–cell coupling but not activation of the inward Cl$^-$ current. Subsequent application of halothane (0.5%), a gap junction channel blocker, rapidly and reversibly uncouples the cells. Spontane-

In this study, we report a number of novel findings on the regulation of Cx43-based cell–cell communication in fibroblast monolayers. Using a newly developed single-electrode technique in conjunction with dye transfer and biochemical experiments, we have demonstrated that Cx43-based communication is acutely inhibited after stimulation of a subclass of G protein–coupled receptors and characterized the underlying signal transduction events. Given its resistance to PTX, receptor action must be mediated by the G$_{q/11}$ or G$_{12/13}$ subfamily of heterotrimeric G proteins. Regulation of cell–cell communication via G protein signaling has not been systematically examined to date. One relevant example concerns anandamide, an arachidonate derivative, which inhibits gap junctions in astrocytes in a PTX-sensitive manner, but otherwise its mode of action is unknown (Venance et al., 1995).

We find that G protein–induced gap junction closure cannot be explained by known second messengers nor by the membrane depolarization that consistently accompanies gap junction closure. Our results obtained with the Rho-inactivating C3 toxin also rule out a role for receptor-mediated Rho signaling in gap junction closure. Previous studies have assigned a central role to PKC and MAP kinase in the regulation of Cx43-based communication (Kanemitsu and Lau, 1993; Hii et al., 1994; for review see Goodenough et al., 1996), while MAP kinase can phosphorylate Cx43 in vitro (Warn-Cramer et al., 1996). However, the lack of effect of phorbol ester, PKC inhibitors, PTX, and 8Br-cAMP strongly argues against the involvement of these Ser/Thr kinases in agonist-induced gap junction closure in Rat-1 fibroblasts. That MAP kinase does not mediate gap junction closure in Rat-1 cells is reinforced by the finding that EGF, a strong activator of the Ras-MAP kinase pathway (van Corven et al., 1993; Hordijk et al., 1994*a*; Kranenburg et al., 1997) has only a minor effect on cell–cell coupling (Fig. 5, *B* and *C*).

Instead, it appears that a c-Src tyrosine kinase pathway links G protein–coupled receptors to gap junction closure. This conclusion is based on the following findings. First, G protein–mediated gap junction closure is prevented by tyrosine kinase inhibitors (tyrphostin 25 and 47) but not by the Ser/Thr kinase inhibitor stauroporine, while it can be mimicked by pervanadate, a tyrosine phosphatase inhibitor; also in hamster fibroblasts, pervanadate (but not other phosphatase inhibitors) decreases cell–cell communication (Husoy et al. 1993). Second, G protein–mediated gap junction closure is accompanied by rapid activation of c-Src (Chen et al., 1994; van Biesen et al., 1996; Dikic et al., 1996; Rodriguez-Fernandez and Rozengurt, 1996; Kranenburg et al., 1997). Third, expression of constitutively active Src inhibits communication. Fourth, dominant-negative c-Src

ous evaporation of halothane from the medium leads to gradual reopening of gap junctions. (*D*) Current responses in fibroblasts derived from Src-deficient mice versus control fibroblasts before (*left*) and after (*right*) treatment with LPA. In control cells, LPA increases the input resistance approximately fivefold, accompanied by a reduction in the relaxation time constant; in Src-deficient cells, LPA fails to evoke detectable changes in the electrical characteristics of the monolayer (although LPA does induce an inward current; not shown). Voltage pulse: 10 mV; holding potential: −70 mV.
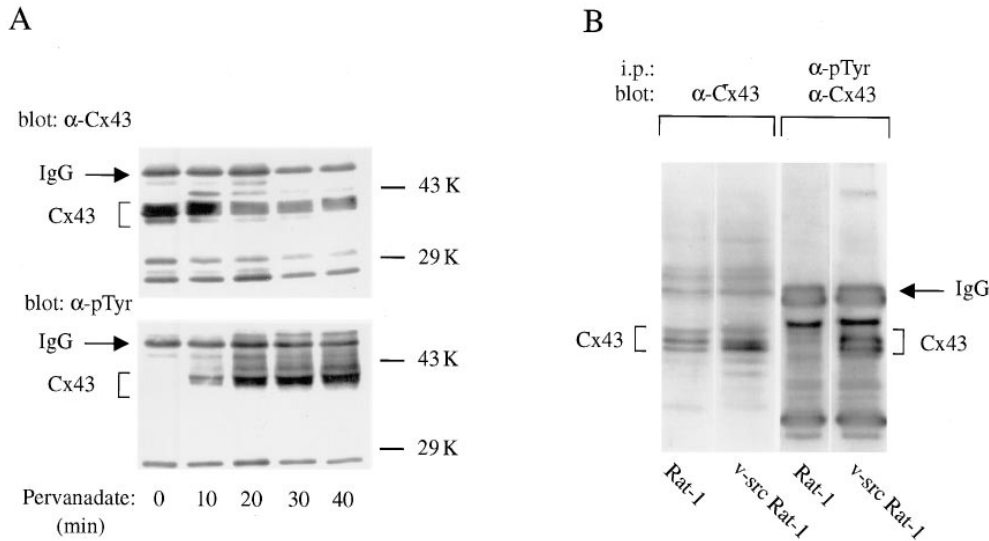
A

blot: α-Cx43

IgG →
Cx43 [

— 43 K

— 29 K

blot: α-pTyr

IgG →
Cx43 [

— 43 K

— 29 K

Pervanadate: 0 10 20 30 40
(min)

B

i.p.:   α-pTyr
blot: α-Cx43   α-Cx43

Cx43 [← IgG

                        ] Cx43

Rat-1   v-src Rat-1   Rat-1   v-src Rat-1

Figure 11. Tyrosine phosphorylation of Cx43 in Rat-1 cells. (*A*) Pervanadate-induced tyrosine phosphorylation of Cx43 as measured by probing immunoprecipitated Cx43 with antiphosphotyrosine antibody in Western blot. Time points indicate minutes after pervanadate addition. Concentrations used: vanadate, 0.4 mM; H_2O_2, 4.8×10^{-4}% (140 nM). (*B*) Cx43 expression (*left two lanes*) and Cx43 tyrosine phosphorylation (*right two lanes*) in normal and v-Src–expressing Rat-1 cells.

protects gap junctions from being closed by G protein–coupled receptors. Finally, agonist-induced gap junction closure is not observed in Src-deficient fibroblasts. The latter observation is of note since one might have anticipated that other Src family members, notably Fyn or Yes, would compensate for the lack of c-Src.

How does activation of the G protein–Src kinase pathway lead to inhibition of Cx43 function? One attractive possibility is that inhibition is due to Src-mediated tyrosine phosphorylation of Cx43. Indeed, enhanced tyrosine phosphorylation of Cx43, correlating with loss of communication, is readily detectable in both v-Src–expressing and vanadate-treated cells (Fig. 11, *A* and *B*). Furthermore, it has been shown that mutation of a specific tyrosine residue in Cx43 (Tyr265) abolishes both inhibition of communication and tyrosine phosphorylation induced by v-Src in a *Xenopus* oocyte expression system (Swenson et al., 1990). The finding that Src family kinases are enriched in cell–cell contacts (Tsukita et al., 1991) would be consistent with a direct action of Src kinases on Cx43. However, we have not yet been able to detect enhanced tyrosine phosphorylation of Cx43 in response to receptor stimulation. While this failure may well be due to technical limitations (e.g., low stoichiometry of phosphorylation or the transient nature of such phosphorylation event), it remains possible that c-Src acts in a more indirect manner, not involving tyrosine phosphorylation of Cx43. The possibility that enhanced serine phosphorylation of Cx43 is involved in gap junction closure deserves some discussion. Serine phosphorylation of Cx43 is thought to regulate intracellular trafficking of Cx43 and correlates with gap junction assembly and maintenance (Musil and Goodenough, 1991; Goodenough et al., 1996). In addition, gap junction closure is often accompanied by enhanced serine phosphorylation of Cx43, which gives rise to a reduced electrophoretic mobility of the protein (for example see Kanemitsu and Lau, 1993; Hii et al., 1994). Although we do detect agonist-induced mobility shifts of Cx43 in Western blots, our analysis reveals that there is no simple correlation between these mobility shifts (which occur relatively slowly) and gap junction closure as judged by kinetic and pharmacological criteria (Giepmans, B.N.G., unpublished observations).

The present study also addresses the mechanism responsible for the gradual recovery of communication occurring in the continuous presence of agonist. Such recovery is commonly observed in response to receptor stimulation. By taking advantage of a truncated, desensitization-defective NK2 receptor, we find that recovery of Cx43-based communication is controlled in large part at the level of receptor desensitization, which in turn is regulated by ligand-induced Ser/Thr phosphorylation of the receptor's COOH-terminal tail (Alblas et al., 1995, 1996). Mutant NK2 receptor not only mediates prolonged uncoupling, but it also mediates ligand-induced morphological transformation, as indicated by the deregulated, criss-cross growth pattern that is observed after NKA addition to mutant NK2 receptor-expressing Rat-1 cells (Alblas et al., 1996). Thus, there is a striking correlation between the duration of junctional uncoupling and phenotypic transformation after (mutant) receptor stimulation, although cause-effect relationships remain to be established.

It is tempting to speculate that temporary inhibition of junctional communication is critical during normal wound healing: after traumatic injury cells at the wound margin are acutely exposed to agonists, including platelet-derived LPA, thrombin, and endothelin, which shut off cell–cell communication to prevent intercellular "leakage" of signaling molecules. In other words, by rapidly closing their gap junctions cells at the wound edge may not arouse their quiescent neighbors. Further experiments are needed to test this model. Receptor-mediated isolation of individual cells from surrounding cells may also be relevant to the concept of compartmental boundaries during embryonic development (Kalimi and Lo, 1989; Godwin et al., 1993). Several outstanding questions remain to be addressed. In particular, what is the identity of the G protein subunit(s) that mediate(s) gap junction closure? What is the nature of the responsible G protein–linked effector(s)? And, does c-Src act in a direct or indirect manner on Cx43? These issues are currently under investigation.

References

Alblas, J., I. van Etten, A. Khanum, and W.H. Moolenaar. 1995. C-terminal truncation of the neurokinin-2 receptor causes enhanced and sustained agonist-induced signaling. *J. Biol. Chem.* 270:8944–8951.

Alblas, J., I. van Etten, and W.H. Moolenaar. 1996. Truncated, desensitization-defective neurokinin receptors mediate sustained MAP kinase activation, cell growth and transformation by a Ras-independent mechanism. *EMBO (Eur. Mol. Biol. Organ.) J.* 15:3351–3360.

Atkinson, M.M., A.S. Menko, R.G. Johnson, J.R. Sheppard, and J.D. Sheridan. 1981. Rapid and reversible reduction of junctional permeability in cells infected with a temperature-sensitive mutant of avian sarcoma virus. *J. Cell Biol.* 91:573–578.

Azarnia, R., S. Reddy, T.E. Kmiecik, D. Shalloway, and W.R. Loewenstein. 1988. The cellular src gene product regulates junctional cell-to-cell communication. *Science.* 239:398–401.

Azarnia, R., M. Mitcho, D. Shalloway, and W.R. Loewenstein. 1989. Junctional intercellular communication is cooperatively inhibited by oncogenes in transformation. *Oncogene.* 4:1161–1168.

Bennett, M.V.L., L.C. Barrio, T.A. Bargiello, D.C. Spray, E. Hertzberg, and J.C. Saez. 1991. Gap junctions: new tools, new answers, new questions. *Neuron.* 6:305–320.

Beyer, E.C. 1993. Gap junctions. *Int. Rev. Cytol.* 137C:1–37.

Bigiani, A., and S.D. Roper. 1995. Estimation of the junctional resistance between electrically coupled receptor cells in *Necturus* taste buds. *J. Gen. Physiol.* 106:705–725.

Bockholt, S.M., and K. Burridge. 1995. An examination of focal adhesion formation and tyrosine phosphorylation in fibroblasts isolated from src-, fyn-, and yes- mice. *Cell Adhes. Commun.* 3:91–100.

Broome, M.A., and T. Hunter. 1996. Requirement for c-Src catalytic activity and the SH3 domain in platelet-derived growth factor BB and epidermal growth factor mitogenic signaling. *J. Biol. Chem.* 271:16798–16806.

Burghardt, R.C., R. Barhoumi, T.C. Sewall, and J.A. Bowen. 1995. Cyclic AMP induces rapid increases in gap junction permeability and changes in the cellular distribution of connexin43. *J. Membr. Biol.* 148:243–253.

Chen, Y.H., J. Pouyssegur, S.A. Courtneidge, and E. Van Obberghen-Schilling. 1994. Activation of Src family kinases by the G protein-coupled thrombin receptor in growth-responsive fibroblasts. *J. Biol. Chem.* 269:27372–27377.

Crow, D.S., E.C. Beyer, D.L. Paul, S.S. Kobe, and A.F. Lau. 1990. Phosphorylation of connexin43 gap junction protein in uninfected and Rous sarcoma virus-transformed mammalian fibroblasts. *Mol. Cell. Biol.* 10:1754–1763.

Dikic, I, G. Tokiwa, S. Lev, S.A. Courtneidge, and J. Schlessinger. 1996. A role for Pyk2 and src in linking G-protein-coupled receptors with MAP kinase activation. *Nature.* 383:547–550.

Eckert, R., A. Dunina-Barkovskaya, and D.F. Huelser. 1993. Biophysical characterization of gap-junction channels in HeLa cells. *Pfluegers Arch.* 424:335–342.

El-Fouly, M.H., J.E. Trosko, and C.C. Chang. 1987. Scrape-loading and dye transfer. A rapid and simple technique to study gap junctional intercellular communication. *Exp. Cell Res.* 168:422–430.

Filson, A.J., R. Azarnia, E.C. Beyer, W.R. Loewenstein, and J.S. Brugge. 1990. Tyrosine phosphorylation of gap junction protein correlates with inhibition of cell-to-cell communication. *Cell Growth Diff.* 1:661–668.

Godwin, A.J., L.M. Green, M.P. Walsh, J.R. McDonald, D.A. Walsh, and W.H. Fletcher. 1993. In situ regulation of cell-cell communication by the cAMP-dependent protein kinase and protein kinase C. *Mol. Cell. Biochem.* 127/128:293–307.

Goldberg, G.S., and A.F. Lau. 1993. Dynamics of connexin43 phosphorylation in pp60[v-src]-transformed cells. *Biochem. J.* 295:735–742.

Goodenough, D.A., J.A. Goliger, and D.L. Paul. 1996. Connexins, connexons, and intercellular communication. *Annu. Rev. Biochem.* 65:475–502.

Hii, C.S.T., S.-Y. Oh, S.A. Schmidt, K.J. Clark, and A.W. Murray. 1994. Lysophosphatidic acid inhibits gap-junctional communication and stimulates phosphorylation of connexin-43 in WB cells: possible involvement of the mitogen-activated protein kinase cascade. *Biochem. J.* 303:475–479.

Hordijk, P.L., I. Verlaan, E.J. van Corven, and W.H. Moolenaar. 1994a. Protein tyrosine phosphorylation induced by lysophosphatidic acid in Rat-1 fibroblasts. *J. Biol. Chem.* 269:645–651.

Hordijk, P.L., I. Verlaan, K. Jalink, E.J. van Corven, and W.H. Moolenaar. 1994b. cAMP abrogates the p21[ras]-MAP kinase pathway in fibroblasts. *J. Biol. Chem.* 269:3534–3538.

Hotz-Wagenblatt, A., and D. Shalloway. 1993. Gap junctional communication and neoplastic transformation. *Crit. Rev. Oncog.* 4:541–558.

Husoy, T., S.O. Mikalsen, and T. Sanner. 1993. Phosphatase inhibitors, gap junctional intercellular communication and ^{125}I-EGF binding in hamster fibroblasts. *Carcinogenesis.* 14:2257–2265.

Jalink, K., and W.H. Moolenaar. 1992. Thrombin receptor activation causes rapid neural cell rounding and neurite retraction independent of classic second messengers. *J. Cell Biol.* 118:411–419.

Jalink, K., T. Hengeveld, S. Mulder, F.R. Postma, M.-F. Simon, H. Chap, G.A. van der Marel, J.H. van Boom, W.J. van Blitterswijk, and W.H. Moolenaar. 1995. Lysophosphatidic acid-induced Ca^{2+} mobilization in human A431 cells: structure-activity analysis. *Biochem. J.* 307:609–616.

Kahn, R.A. 1991. Fluoride is not an activator of the smaller (20-25 kD) GTP-binding proteins. *J. Biol. Chem.* 266:15595–15597.

Kalimi, G.H., and C.W. Lo. 1989. Communication compartments in the gastrulating embryo. *J. Cell Biol.* 107:241–255.

Kanemitsu, M.Y., and A.F. Lau. 1993. Epidermal growth factor stimulates the disruption of gap junctional communication and connexin43 phosphorylation independent of 12-O-tetradecanoyl-phorbol 13-acetate-sensitive protein kinase C: the possible involvement of mitogen-activated protein kinase. *Mol. Biol. Cell.* 4:827–848.

Kranenburg, O., I. Verlaan, P.L. Hordijk, and W.H. Moolenaar. 1997. G[i]-mediated activation of the Ras-MAP kinase pathway involves a 100 kD tyrosine-phosphorylated Grb2 SH3-binding protein, but not Src nor Shc. *EMBO (Eur. Mol. Biol. Organ.) J.* 16:3097–3105.

Kumar, N.M. and N.B. Gilula. 1996. The gap junction communication channel. *Cell.* 84:381–388.

Lasater, E.M. 1987. Retinal horizontal cell gap junctional conductance is modulated by dopamine through a cAMP-dependent protein kinase. *Proc. Natl. Acad. Sci. USA.* 84:7319–7323.

Lindau, M., and E. Neher. 1988. Patch-clamp techniques for time-resolved capacitance measurements in single cells. *Pfluegers Arch.* 411:137–146.

Machesky, L.M., and A. Hall. 1996. Rho: a connection between membrane signaling and the cytoskeleton. *Trends Cell Biol.* 6:304–310.

Maldonado, P.E., B. Rose, and W.R. Loewenstein. 1988. Growth factors modulate cell-to-cell communication. *J. Membr. Biol.* 106:203–210.

Mesnil, M., V. Kurtovskikh, C. Piccoli, C. Elfgang, O. Traub, K. Willecke, and H. Yamasaki. 1995. Negative growth control of HeLa cells by connexin genes: connexin species specificity. *Cancer Res.* 55:629–639.

Moolenaar, W.H., O. Kranenburg, F.R. Postma, and G.C.M. Zondag. 1997. Lysophosphatidic acid: G protein signaling and cellular responses. *Curr. Opin. Cell Biol.* 9:168–173.

Musil, L.S., and D.A. Goodenough. 1991. Biochemical analysis of connexin43 intracellular transport, phosphorylation and assembly into gap junction plaques. *J. Cell Biol.* 115:1357–1374.

Paul, D.L. 1995. New functions for gap junctions. *Curr. Opin. Cell Biol.* 7:665–672.

Postma, F.R., K.J. Jalink, T. Hengeveld, A.G.M. Bot, J. Alblas, H.R. de Jonge, and W.H. Moolenaar. 1996. Serum-induced membrane depolarization in quiescent fibroblasts: activation of a chloride conductance through the G protein-coupled LPA receptor. *EMBO (Eur. Mol. Biol. Organ.) J.* 15:63–72.

Rae, J., K. Cooper, P. Gates, and M. Watsky. 1991. Low access resistance perforated patch recordings using amphotericin B. *J. Neurosci. Methods.* 37:15–26.

Ridley, A.J., and A. Hall. 1992. The small GTP-binding protein rho regulates the assembly of focal adhesions and actin stress fibers in response to growth factors. *Cell.* 70:389–399.

Roche, S., M. Koegl, M.V. Barone, M.F. Roussel, and S.A. Courtneidge. 1995. DNA synthesis induced by some but not all growth factors requires Src family protein tyrosine kinases. *Mol. Cell. Biol.* 15:1102–1109.

Rodriguez-Fernandez, J.L., and R. Rozengurt. 1996. Bombesin, bradykinin, vasopressin, and phorbol esters rapidly and transiently activate Src family tyrosine kinases in Swiss 3T3 cells. *J. Biol. Chem.* 271:27895–27901.

Spray, D.C. 1994. Physiological and pharmacological regulation of gap junction channels. *In* Molecular Mechanisms of Epithelial Cell Junctions: From Development to Disease. S. Siti, editor. R.G. Landes Company, Austin, TX. 195–215.

Swenson, K.I., H. Piwnica-Worms, H. McNamee, and D.J. Paul. 1990. Tyrosine phosphorylation of the gap junction protein connexin43 is required for the pp60[v-src]-induced inhibition of communication. *Cell Regul.* 1:989–1002.

Tsukita, S., K. Oishi, T. Akiyama, Y. Yamanashi, T. Yamamoto, and S. Tsukita. 1991. Specific proto-oncogenic tyrosine kinases of src family are enriched in cell-to-cell adherens junctions where the level of tyrosine phosphorylation is elevated. *J. Cell Biol.* 113:867–879.

Van Biesen, T., L.M. Luttrell, B.E. Hawes, and R.J. Lefkowitz. 1996. Mitogenic signaling via G protein-coupled receptors. *Endocr. Rev.* 17:698–714.

Van Corven, E., A. Groenink, K. Jalink, T. Eichholtz, and W.H. Moolenaar. 1989. Lysophosphatidate-induced cell proliferation: identification and dissection of signaling pathways mediated by G proteins. *Cell.* 59:45–54.

Van Corven, E., P.L. Hordijk, R.H. Medema, J. L. Bos, and W.H. Moolenaar. 1993. Pertussis toxin-sensitive activation of p21[ras] by G protein-coupled receptor agonists in fibroblasts. *Proc. Natl. Acad. Sci. USA.* 90:1257–1261.

Van der Valk, J., I. Verlaan, S.W. de Laat, and W.H. Moolenaar. 1987. Expression of pp60[v-src] alters the ionic permeability of the plasma membrane in rat cells. *J. Biol. Chem.* 262:2431–2434.

Venance, L., D. Piomelli, J. Glowinski, and C. Giaume. 1995. Inhibition by anandamide of gap junctions and intercellular calcium signaling in strital astrocytes. *Nature.* 376:590–594.

Warn-Cramer, B.J., P.D. Lampe, W.E. Kurata, M.Y. Kanemitsu, L.W.L. Loo, W. Eckhart, and A.F. Lau. 1996. Characterization of the mitogen-activated protein kinase phosphorylation sites on the connexin-43 gap junction protein. *J. Biol. Chem.* 271:3779–3786.